TRG Report 1279 (C)

UNCLASSIFIED

TRG Report 1279 (C)
Sub-ref.: JNPC-MWP(GSG)/P(66)69

United Kingdom Atomic Energy Authority

THE EFFECT OF A TENSILE RESTRAINT ON GRAPHITE SPECIMENS IRRADIATED IN BR-2

J. E. BROCKLEHURST, A. A. McFARLANE
and B. S. GRAY
Reactor Materials Laboratory
Culcheth

1966

THE REACTOR GROUP
HQ, Risley, Warrington, Lancs

Obtainable from H.M. Stationery Office
Price 4s. 6d. Net

R2228

TRG Report 1279 (C)
Sub-ref: JNPC-MWP(GSG)/P(66)69

THE EFFECT OF A TENSILE RESTRAINT ON GRAPHITE SPECIMENS IRRADIATED IN BR-2

by

J. E. Brocklehurst, A. A. McFarlane and B. S. Gray

SUMMARY

The ability of graphite to absorb strain by plastic deformation under irradiation is important to the design of the core in graphite moderated reactors, as it determines the extent of self-stressing due to the differential irradiation growth caused by flux and temperature gradients.

Specimens of near-isotropic graphites, in the form of rings restrained from shrinking at the inner bore by a mandrel have been irradiated in BR-2, at about 400°C. The net specimen strain rate depended on the rate of irradiation-induced shrinkage and the temperature changes during each reactor cycle.

It is shown that at least 0·6% plastic strain may be absorbed in tension without cracking, even when strain is applied for part of the time at rates 2 to 3 times the normal shrinkage rate. The strength of such specimens is not reduced below the unirradiated value by the presence of creep strain. Temperature transients due to operational difficulties caused the development of radial cracks in some specimens, of which a few failed completely. Thus tensile failure appears to be preceded by the development of such fine cracks.

Draft submitted by Authors: 29 June 1966

This Report relates to work carried out on ADME 206, Task No. 6

Report approved for issue by J. M. Hutcheon, 18 August 1966

C.14

U.D.C. Nos.
661.666.2:539.125.5.04

CONTENTS

INTRODUCTION

1. A knowledge of the plastic behaviour of graphite under stress and fast neutron irradiation is important to the core design of the civil Advanced Gas-Cooled Reactor,[1] in order to estimate the differential stress induced in the moderator by flux and temperature gradients.

2. Experiments on graphite irradiated under constant compressive and tensile stresses in the reactor BR-2 at Mol, Belgium, have been described by Gray, Brocklehurst and McFarlane.[2]

3. This Report gives the results of an additional experiment in BR-2 in which the creep behaviour was studied by restraining the irradiation-induced shrinkage. This experiment was primarily intended to indicate the ability of graphite to absorb plastic strain under more extreme conditions than those existing in the constant-stress experiments.

4. Specimens were included in two creep rigs (4642 and 4635) operating at a nominal temperature of 410°C and were irradiated to peak fast neutron doses of about 18 and 37 x 10^{20} n cm^{-2}.

DESCRIPTION OF THE EXPERIMENT

5. The BR-2 creep rigs have been described by Greenslade and Williams[3] and this experiment was designed to fit a standard capsule. Fig. 1 shows the convoluted steel bellows capsule containing specimens in the form of rings which are restrained from shrinking by a close-fitting central Nimonic 80A mandrel.

6. The size of the capsule limited the diameter of the specimens to 0·38 in. o.d. 0·23 in. i.d. The mandrel is in the form of a tube 0·23 in. o.d., 0·20 in. i.d. carrying 8 such specimens each 0·19 in. long, and lies on the axis of the capsule. The tube supports the end compressive load arising from coolant pressure on the capsule. The bores of the specimens were reamed, and the Nimonic tubes were centreless ground. Thermocouples and neutron dose monitors are also included in the capsule.

7. The capsules are filled with a helium/neon gas mixture and are in direct contact with the reactor coolant. The mean specimen temperature is determined by the gas gap between a graphite sleeve surrounding the specimens and the wall of the capsule, the gas composition, and the mean level of nuclear heating in the graphite. At constant reactor power the specimen temperature varies with time during an irradiation cycle as the distribution of nuclear heating varies, i.e. it is a function of control rod position.

8. As the graphite specimens shrink onto the restraint mandrel under fast neutron irradiation, tensile circumferential stresses build up with a maximum value at the inner diameter of the specimen. A smaller compressive radial stress also develops, having a maximum value at the inner radius and falling to zero at the outer radius.

9. The capsules were located in the top half of the irradiation rig so that the specimen temperature was either substantially constant or was rising during each cycle. This avoids the sudden thermal strain due to differential expansion which would occur on reactor start-up if the capsule was in a position where the specimen temperature fell during an irradiation period.

However, a rise in temperature during irradiation imposes an additional strain on the specimens, and it was considered that, in view of the temperature changes anticipated, the experiment would provide a severe test of the tensile creep behaviour of graphite. Fig. 2 shows the temperature history of each capsule.

ANALYSIS OF STRESSES

10. The stress distribution in thick-walled cylinders under internal or external pressure obtained using elastic theory(4) was used as a basis for design, although it is realised that the non-linear stress/strain behaviour of graphite may significantly affect the stress distribution in the specimen. Thus the elastic equations may not apply in the subsequent analysis of results, but the experiment is of course primarily concerned with the measurement of strain.

11. For the size of specimen considered here, elastic theory yields a circumferential tensile stress at the outer radius which is 54% of that at the inner radius and a variation across the wall as shown in Fig. 3. The radial compressive stress is approximately half the circumferential stress at the inner radius, and falls to zero at the outer surface.

12. Compressive hoop stresses develop in the Nimonic restraint tube and the maximum value is 3·5 times the maximum tensile stress in the graphite. Thus, for a maximum anticipated tensile breaking stress of 4000 lb in^{-2} in the graphite, the compressive stress in the Nimonic will have a maximum value of 14,000 lb in^{-2} which is not expected to produce permanent deformations in this material. (Limit of proportionality in tension ~ 38,000 lb in^{-2} at 400°C).

13. The maximum load applied longitudinally to the Nimonic tube by the bellows is about 55 lb(2) giving a small axial compressive stress of 5500 lb in^{-2}.

14. Thus, essentially, a biaxial stress system is built up in restrained specimens and the major stress is tensile. In specimens which do not fracture, i.e. in which the stresses are relieved by creep, diameter measurements will give the amount of shrinkage restrained, and this will be a maximum at the inner diameter.

GRAPHITES EXAMINED

15. With the exception of the normal P.G.A. graphite (L14), the graphites were improved isotropic materials designated by code letters.(5) Specimens were irradiated in groups of 4 including one control which had sufficient clearance to remain unrestrained. Table I shows that each irradiation capsule contained 2 groups, a total of 8 specimens. Of the 3 restrained specimens of each group in rig No. 4635, two had their axes in a direction parallel to the original block extrusion, and the third in a perpendicular direction. The control specimens and all specimens in rig No. 4642 had their axes in the parallel direction.

16. These graphites were all extruded and, in specimens with cylindrical axes in a direction parallel to extrusion, the tensile hoop stress always acts in a direction perpendicular to extrusion.

EXPERIMENTAL MEASUREMENTS

DIMENSIONAL MEASUREMENTS

17. Inside diameter measurements were made with the internal caliper as described by Brocklehurst, McFarlane and Hall.[6] Several measurements were taken as the specimen was rotated, and results obtained at both ends of the specimen. Settings could be made to ~ 10^{-5} in. but the accuracy was limited by the uniformity of the specimen bore.

18. Outside diameters were measured with a micrometer on all specimens, but a more accurate external caliper method[6] was also used for specimens in rig No.4642, for which the irradiation period was shorter and the diameter changes smaller.

19. Length measurements were also made on some of the annular ring specimens and on the outer graphite sleeves using a normal comparator technique with slip gauges.

20. Diameter measurements with the calipers are expressed as differences from a standard value but were calibrated to give absolute values[6] which are necessary when considering the specimen/restraint gap. The shrinkage restrained depends on the initial clearance gap at the operating temperature, and owing to a differential thermal expansion coefficient between graphite and Nimonic of about 10^{-5} degC^{-1}, a temperature change of 100 degC is equivalent to 0·1% strain. This is approximately the breaking strain of graphite, and hence the initial choice of gap is important.

STRENGTH MEASUREMENTS

21. A number of tests were made on the ring specimens by threading them on a rubber tube and internally pressurising either pneumatically, using the apparatus described by Brocklehurst et al.,[6] or hydraulically, using an apparatus of improved design. The interpretation[6] of the condition for fracture in the ring specimens was deduced from results obtained over a limited range of specimen sizes, and has now been shown to break down beyond this range. Recent unpublished work[7] has shown that the non-linear stress-strain behaviour of graphite has a significant effect on the stress distribution in the ring under internal pressure; this is being examined further. However, in this Report, the test is used as a guide to the effect of creep strain on tensile strength.

22. In another comparative test, a few rings were broken under diametral compression which initiated localised tensile failure at the inner bore on the loaded diameter.[8]

RESULTS

EXAMINATION FOR CRACKS

23. All specimens were examined for cracks on the polished end faces. Table II gives the comments on crack formation for each group of specimens.

24. Figure 4 is a radiograph showing that at least three specimens had cracks passing through at one point in the wall. The specimens were identified by reference scratches on the outer surface where the hoop stress is a minimum, but these reference marks may have caused some stress concentration and contributed to the formation of cracks since in two of these specimens the crack coincided with a reference mark.

25. Microscopic examination of the end faces showed the development of radial cracks in other specimens with 3 or 4 fine cracks on each face, and most of these appeared to start at the inner diameter and usually at a flaw on the circular bore. In some cases these fine cracks appeared to cross the wall. The depth of the fine cracks was not determined, but their effect on the strength of the rings was examined. Figs 5a, b, c and d are photographs of a PI-3 graphite specimen with a major crack, a typical specimen with a developed crack pattern (0·60% shrinkage restrained at i.d.), a restrained specimen with no cracks (0·54% restrained at i.d.) and a control specimen. The concentric rings are shallow scratches on the polished specimen surface which were originally intended for use as measurement references.

DIMENSIONAL CHANGES

26. Table I gives measurements of length and diameter before and after irradiation, the diameter measurements with the calipers being expressed as differences from a standard value. The accuracy of the unirradiated diameter measurements is indicated by the standard deviation of the mean of several readings taken as the specimen is rotated (a typical standard deviation for the i.d. measurements is $\pm$ 40 x 10^{-6} in. or $\pm$ 0·02%). Inside diameter measurements at both ends of the specimen give the amount of taper, which in some cases was about 0·1%.

27. Table III gives the dimensional changes, irradiation doses, and the amount of shrinkage restrained (measured at room temperature) when the shrinkage of restrained specimens is compared with that of the corresponding control. The irradiation temperature for each group of specimens is included in Table II.

STRENGTH TESTS

28. Table IV gives the internal pressure at fracture of individual irradiated specimens, and mean values for unirradiated specimens for which the spread is indicated by the standard deviation. Differences in dimensions between the specimens should not produce more than a 5% variation in the internal pressure required for fracture, and this is smaller than the quoted standard deviations.

29. Table IV also includes the results of the diametral compression test; these are expressed as the product of the diametral load p per unit specimen length and a geometrical factor K to allow for small variations in specimen size.[8] This test was only done on specimens which did not contain visible cracks since the point of failure is predetermined.

30. Mean values for the tensile strength and strain to fracture of unirradiated cylindrical specimens of these graphites are also given for comparison.

DISCUSSION

DIMENSIONAL CHANGES

31. Figure 6 shows agreement between the length changes of outer sleeves and unrestrained rings of isotropic graphite (giving changes parallel to extrusion) and other data[2] from BR-2 creep capsules irradiated at the same nominal temperature. Ring diameter measurements (perpendicular to extrusion) tend to show a smaller shrinkage at high doses.

32. Figure 7 shows the shrinkage of restrained isotropic graphite specimens at the inner diameter in comparison with the corresponding controls, and Fig. 8 shows the shrinkage restrained at both the inner and outer diameters. Some scatter is inevitable because of variations in the initial specimen/restraint gap. It is seen that > 0·6% shrinkage is restrained at the inner bore and some specimens show an increase in internal diameter due to thermal straining. In particular, for the high-dose isotropic graphite specimens which did not show any crack formation, the shrinkage restrained at the inner diameter was 0·54 - 0·60%. The shrinkage restrained at the outer diameter, which is less accurate owing to the surface finish, is about half that at the inner diameter; this is nearly the same ratio as that of the corresponding hoop stresses calculated from elastic theory (Fig. 3).

33. The axial shrinkage of restrained isotropic graphite specimens is greater than that of the controls, and the difference in some cases appears to be greater than can be accounted for by a Poisson's ratio effect.

34. Figure 9 shows that the length measurements on the P.G.A. graphite control specimens agree with previous data[2] on parallel-cut P.G.A. graphite from BR-2 creep capsules. Diameter measurements on these two specimens are, however, inconsistent. The inside diameter apparently shrinks considerably more than the outside, but Table I shows that, for the lower-dose specimen, the non-uniformity of the specimen gives rise to a large uncertainty in these measurements and the error is sufficient to explain the discrepancy. The reason for the difference between the diameter measurements on the higher-dose P.G.A. specimen is not clear, and for both these samples the mean of the two diameter readings has been taken as the unrestrained shrinkage and is shown in Fig. 9 with previous P.G.A. perpendicular data[2] from BR-2 creep capsules. Fig. 10 shows the inner-diameter shrinkage of the restrained P.G.A. compared with the unrestrained data and Fig. 11 shows the amount of shrinkage restrained at both diameters, which again is > 0·6% at the inner diameter with a lower value at the outer diameter.

STRENGTH

35. From the results of the internal pressure test, Table IV shows that creep strains up to about ½% at the inner bore of specimens for which there were no visible cracks, do not produce large reductions in strength. The most noticeable effect is observed in specimens containing fine radial cracks (similar to Fig. 5b) which can, but do not necessarily, reduce the strength below the unirradiated value. The low result for the control specimen 2K is probably due to a flaw in the specimen.

36. These conclusions are supported by the diametral test on a few specimens without visible cracks, again showing that creep strains up to 0·3% at the inner bore have no drastic effect on strength.

CRACK FORMATION

37. The presence of a fine crack structure suggests that, at some stage, the graphite was subjected to strains such that the specimen was only marginally below the point of complete fracture. Thus complete failure appears to be preceded by an increase in the number and/or length of such fine cracks, and this has more recently been supported by the work of Taylor et al.[9] We must, however, consider why the cracks develop and in particular why the specimens in group 4 show no cracks, while those of the same graphite in group 5, at a slightly higher dose, but apparently more stable temperature conditions, show the development of a crack structure.

38. One difference between the specimens of groups 4 and 5 is the initial specimen/restraint gap, given in Table III. Owing to the smaller initial gap and higher operating temperature of group 5 specimens, a larger fraction of the irradiation-induced shrinkage would meet restraint. However, to argue that this explains the difference between specimens in groups 4 and 5 suggests a strain limit < 0·6% and it has already been shown [2,10] that similar graphites will absorb > 0·6% tensile strain by irradiation-induced creep without any signs of fracture. It seems likely, therefore, that the strain rate is the important factor and the following argument supports this.

39. The strain rate of the specimens was considerably increased above the normal graphite shrinkage rate by the rise in temperature during the irradiation, owing to the differential thermal expansion at the graphite/restraint interface (about 0·1% per 100 degC). Fig. 2 shows the temperature history of the capsules, but it should be noted that difficulties with control rod operation caused temperature transients, giving instantaneous changes. In one case, the transient was particularly severe, giving a temperature increase of 60 degC to specimens in groups 1 and 2, 40 degC to those in groups 3 and 4, and 20 degC to those in groups 5 and 6. Fig. 12 summarises the temperature transients during the latter half of the irradiation of rig No. 4635 and these could make an important contribution to the formation of cracks, depending on the elastic strain in the specimens immediately prior to the transient.

40. By considering the graphite shrinkage rate, and the temperature changes at different stages in each capsule, it is possible to estimate the total strain rate applied to the specimens. Hence, assuming that equilibrium conditions exist, and a value of the creep constant from constant-stress experiments,[2] it is possible to estimate the stress and elastic strain in the graphite.

41. Thus, after an initial period the shrinkage rate of control specimens is 0·025% per 10^{20} n cm^{-2} and we will assume that all shrinkage at the bore is restrained. Fig. 7 shows that this general assumption is reasonable for specimens in rig No. 4635.

42. Consider the temperature changes in Fig. 2 during the later stages of the irradiation of rig No.4635. At the beginning of each reactor cycle, the irradiation temperature of specimens in capsules 21 and 22 (groups 1-4) is about 100 degC lower than at the end of the previous cycle, and these specimens therefore have a thermal strain relief of ~ 0·1%; some time is therefore required during the initial part of each cycle to build up the elastic strain

again. Specimens in capsule 23 (groups 5 and 6) start each cycle at the same temperature as at the end of the previous one; hence there is no thermal relief and the net thermal and shrinkage strain rate has to be accommodated by creep almost immediately.

43. Now the rate of thermal strain in the initial stages of each cycle in capsule 23 is similar to that during the later stages of each cycle for capsule 22, viz. $\simeq$ 0·04% per 10^{20} n cm^{-2}. Hence, the net strain rates are also similar, 0·065% per 10^{20} n cm^{-2}, and using a creep constant given by Gray et al.[2] of $0 \cdot 17 \times 10^{-6}$ $(10^{20}$ n $cm^{-2})^{-1}$ (lb $in^{-2})^{-1}$ and assuming linearity with stress, the equilibrium circumferential stress at the inner diameter of the specimen $\simeq$ 4000 lb in^{-2} and must be near the fracture stress. The conditions considered exist during the initial part of a cycle for specimens in group 5 and during the final part of the cycle for specimens in group 4; hence the effect of a transient temperature rise will depend on the position in the cycle at which it occurs.

44. In the initial stages of a cycle, the additional thermal strain due to a transient will have a greater effect on capsule 23 than capsule 22, and a transient at the end of a cycle would have a greater effect on capsule 22 than capsule 23.

45. Fig. 12 shows that the major transients in the latter half of the irradiation occurred in the first few days of each cycle and therefore affected the specimens in group 5 more than those in group 4, even though the thermal change was smaller, i.e. the additional 0·02% might be sufficient to initiate cracks in specimens in group 5 if applied instantaneously when the elastic strain is already high, but a higher thermal strain imposed on group 4 specimens at the same time would not have an important effect, since the elastic strain in these specimens would be comparatively low.

46. From the 3 specimens which showed a complete crack through the wall (Fig. 4), an estimate of the crack width suggests that these specimens failed approximately 4-6 cycles before the end of the irradiation; the largest transient shown in Fig. 12 and discussed previously occurred 4 cycles from the end.

47. The evidence suggests, therefore, that the observed cracks were initiated during a temperature transient, this being the only way one can explain why group 4 specimens remain uncracked. Thus, provided that instantaneous strains are not superimposed, the specimens can absorb strain which on average is equal to the natural shrinkage (also demonstrated by Gray et al.[2] for specimens under constant tensile load) but this experiment also shows that the graphite can withstand, at least for part of the time, a strain rate 2-3 times greater than the natural shrinkage rate of the unstressed graphite.

CONCLUSIONS

48. A number of polycrystalline isotropic graphites in the form of rings restrained from shrinking at the inner bore have been irradiated at $\simeq$ 400°C. It is shown that at least 0·6% plastic strain may be absorbed in tension without cracking, even when strain is applied for part of the time at rates 2 to 3 times the normal shrinkage rate. The presence of creep strain alone at this level does not seriously reduce the tensile strength of graphite (values are certainly still above the unirradiated value).

49. Cracks observed in some specimens almost certainly developed during temperature transients when an additional instantaneous strain was imposed on the specimens. The presence of fine cracks does not necessarily reduce the strength of the graphite below the unirradiated value, and complete tensile failure appears to be preceded by the development of such cracks.

REFERENCES

1. NETTLEY, P. T., BRIDGE, H., and SIMMONS, J. H. W. Irradiation behaviour of graphite. J. Brit. Nucl. En. Soc., April 1963, p.267.

2. GRAY, B. S., BROCKLEHURST, J. E., and McFARLANE, A. A. Irradiation-induced plasticity in graphite. 1966. TRG Report 1071(C).

3. GREENSLADE, G. K., and WILLIAMS, R. Graphite irradiation rigs in BR-2 for examination of dimensional change and creep properties. TRG Report 821(R). To be published.

4. TIMOSHENKO, S. Strength of materials, Pt. II. Van Nostrand Co.

5. HANSTOCK, R. F. Internal document.

6. BROCKLEHURST, J. E., McFARLANE, A. A., and HALL, E. Methods of measuring tensile strength and dimensional changes of small graphite ring specimens. 1965. TRG Report 1020(C).

7. WITT, F. J., Oak Ridge National Laboratory, U.S.A. Private communication

8. BROCKLEHURST, J. E., and GILCHRIST, K. E. Unpublished work.

9. TAYLOR, R., et al. The mechanical properties of reactor graphite. To be published

10. PERKS, A. J., and SIMMONS, J. H. W. Dimensional changes and radiation creep of graphite at very high neutron doses. Carbon, 1966, vol. 4, pp.35-98.

TABLE I   Measurements on Restrained Graphite Ring Specimens in BR-2 Rigs 4635 and 4642

Rig no.	Capsule no.	Nimonic tube dia. in.	Specimen: Group	Specimen: Code	Specimen: Type	Graphite	Before irradiation: Length l_0 in.	Before irradiation: Direct O.D. in x 10^4 (mean of 8) $\pm \sigma_m$	Before irradiation: Difference from standard, in x 10^6: O.D. Standard =0.3668 in.: Top (mean of 8) $\pm \sigma_m$	Before irradiation: O.D. Standard =0.3668 in.: Reverse (mean of 8) $\pm \sigma_m$	Before irradiation: I.D. Standard =0.22433 in.: Top (mean of 8) $\pm \sigma_m$	Before irradiation: I.D. Standard =0.22433 in.: Reverse (mean of 8) $\pm \sigma_m$	After irradiation: Length l_1 in.	After irradiation: Direct O.D. in x 10^4 (mean of 8)	After irradiation: Differences from standard, in x 10^6: O.D. Standard =0.3668 in.: Top (mean of 8)	After irradiation: O.D. Standard =0.3668 in.: Reverse (mean of 8)	After irradiation: I.D. Standard =0.22433 in.: Top (mean of 8)	After irradiation: I.D. Standard =0.22433 in.: Reverse (mean of 8)
4635	21	0.2311		BMO	Outer sleeve	P13	2.019441						2.010309					
			1	1A	spec.	L14		3794 ± 1			7874 ± 16	7989 ± 11		3783			7604	7677
				C	control	"	0.185965	3790 ± 2			12635 ± 189	13122 ± 164	0.184613	3776, 8			11142	11434
				L	spec.	" *	0.19665	3795 ± 1			7680 ± 13	7693 ± 7	0.19580	3785			7615	7593
				B	"	"		3795 ± 1			7673 ± 27	7565 ± 22		3790			7512	7569
			2	D	"	PH2		3794 ± 1			7563 ± 38	7595 ± 25		3785			7547	7529
				K	control	"	0.194615	3797 ± 1			12508 ± 29	12528 ± 18	0.193704	3782			11522	11517
				N	spec.	" *	0.1912	3792 ± 2			7822 ± 27	7833 ± 12	[illegible]19008	3786			7581	7630
				E	"	"		3794 ± 1			7221 ± 61	7502 ± 45		3786			7554	7591
	22	0.2310		BMP	Outer sleeve	P13	2.015889						2.001987					
			3	2A	spec.	L14		3787 ± 2			7577 ± 86	7768 ± 58		3777			7580	7542
				C	control	"	0.193436	3789 ± 1			12663 ± 45	12516 ± 24	0.191042	3771, 69			10569	10665
				L	spec.	" *	0.1848	3791 ± 1			7696 ± 70	7847 ± 70	0.18340	3779			7831	7763
				B	"	"		3787 ± 1			8016 ± 59	7964 ± 29		-			-	-
			4	D	"	P13		3797 ± 1			7721 ± 7	7676 ± 11		3787			7321	7360
				K	control	"	[illegible]191381	3797 ± 1			12694 ± 11	12496 ± 50	0.190127	3773			10901	10988
				H	spec.	" *	0.1967	3795 ± 1			7546 ± 14	7520 ± 21	0.19523	3785			7305	7320
				E	"	"		3799 ± 1			7649 ± 18	7761 ± 11		3786			7332	7352
	23	0.2313		BMR	Outer sleeve	P13	2.018724						2.002591					
			5	3A	spec.	"		3803 ± 1			7585 ± 70	7917 ± 52		-			-	-
				C	control	"	[illegible]190973	3795 ± 1			12571 ± 31	12505 ± 38	0.189573	3772			11085	10970
				L	spec.	" •	[illegible]1909	3797 ± 1			7748 ± 54	7612 ± 44	0.18940	3785			7685	7569
				B	"	"		3798 ± 1			7739 ± 77	7880 ± 43		3785			7717	7746
			6	D	"	PH2		3795 ± 1			7746 ± 11	7790 ± 25		3784			7750	7757
				K	control	"	0.189697	3792 ± 1			12724 ± 43	12678 ± 34	0.188207	3772			11229	11093
				N	spec.	" *	0.1875	3804 ± 1			7518 ± 11	7536 ± 9	0.18589	3793			7690	7688
				E	"	"		3792 ± 1			7802 ± 20	7869 ± 32		-			-	-
4642	27	0.2312		CNT	Outer sleeve	P15	2.027149						2.018705					
			7	COV	spec.	PP		3755 ± 0.8	8063 ± 83	8837 ± 56	7640 ± 21	7604 ± 13		3751	7751	8644	7455	7471
				COF	control	"	0.189729	3735 ± 1.0	-	-	12656 ± 8	12501 ± 10	0.189346	3727	-	-	12031	11843
				COW	spec.	"		3785 ± 0.3	11557 ± 19	11656 ± 23	7678 ± 21	7651 ± 22		3782	11221	11371	7544	7513
				COX	"	"		3787 ± 0.2	11517 ± 39	11753 ± 32	8164 ± 28	8342 ± 29		3781	11103	11253	7660	7897
			8	COR	"	PO		3813 ± 0.3	14620 ± 22	14000 ± 19	7534 ± 17	7574 ± 23		3810	14385	13807	7557	7512
				COE	control	"	0.190013	3765 ± 0.4	9565 ± 47	9472 ± 20	13305 ± 68	13192 ± 75	0.189645	3757	8936	8829	12633	12417
				COS	spec.	"		3800 ± 0.4	13242 ± 13	13185 ± 17	7541 ± 11	7547 ± 21		3800	13197	13063	7536	7526
				COT	"	"		3794 ± 0.6	12753 ± 31	12102 ± 22	8268 ± 18	8592 ± 57		3788	12121	11476	7711	7923
	28	0.2308		CNV	Outer sleeve	P15	2.021722						-					
			9	COK	spec.	"	0.19129	3805 ± 0.2	13534 ± 29	13618 ± 13	7703 ± 9	7685 ± 15	0.19060	3799	13009	13074	7236	7249
				COC	control	"	0.188192	3801 ± [illegible]5	13217 ± 23	13233 ± 20	12620 ± 16	12613 ± 11	0.187862	3794	12527	12539	12076	11909
				COL	spec.	"	0.19115	3798 ± 0.2	12735 ± 11	12974 ± 11	7687 ± 18	7702 ± 12	0.19057	3793	12293	12539	7264	7300
				COM	"	"	0.19112	3809 ± 0.1	14099 ± 22	13725 ± 18	8329 ± 21	8513 ± 53	0.19059	3801	13327	12972	7852	7889
			10	CON	"	PH3	0.19153	3798 ± 0.2	12683 ± 24	12631 ± 15	7804 ± 11	7755 ± 24	0.19063	3790	12022	12090	7344	7315
				COD	control	"	0.187804	3796 ± [illegible]5	12618 ± 23	12429 ± 20	13012 ± 90	12616 ± 96	0.187324	3786	11783	11615	12348	11945
				COO	spec.	"	0.19317	3789 ± 0.2	12014 ± 58	11609 ± 22	7586 ± 8	7588 ± 15	0.19234	3781	11474	11137	7230	7254
				COP	"	"	0.19208	3774 ± 0.6	10503 ± 28	10015 ± 21	8322 ± 33	8166 ± 50	0.19145	3763	9804	9302	7669	7485

* Indicates cylindrical axis of specimen is perpendicular to extrusion; all other specimens have their axis parallel

TABLE II

Crack Formation in Restrained Specimens

Group	Graphite	Mean fast neutron dose, $n.cm^{-2}$	Irradiation temperature °C	Comments on radial crack formation
1	L14	22.5×10^{20}	340 ± 70	Fine cracks observed
2	PH2	24.5	"	" " "
3	L14	31.8	370 ± 40	" " " 1 specimen with large crack *
4	PI3	33.2	"	No cracks observed
5	PI3	36.6	420 ± 20	Fine cracks observed, 1 specimen with large crack
6	PH2	36.9	"	" " " 1 specimen with large crack *
7	PP	15.1	320 ± 40	No cracks observed
8	PO	15.7	"	No cracks observed
9	PI5	17.4	360 ± 20	" " "
10	PH3	17.7	"	" " "

* Major crack coincides with reference mark on outside of specimens

TABLE III

Shrinkage of Graphite Ring Specimens
in BR-2 Rigs 4635 and 4642

Specimen Group	Specimen Code	Graphite	Fast neutron dose $n.cm^{-2}$	Initial gap (on dia.) in x 10^4 Top	Initial gap Reverse	Shrinkage % I.D. Top	I.D. Reverse	I.D. Mean	O.D. Top	O.D. Reverse	O.D. Mean	O.D. (micrometer)	Length	Shrinkage restrained (measured at room temp.) I.D. %	O.D. %
1	1A	L14	21.7 x 10^{20}	11	12	0.116	0.134	0.125				0.29		0.39^{+}	0.22^{+}
	C	" (control)	22.2	59	63	0.630	0.711	0.670				0.32, 0.37	0.730	-	-
	L	" *	22.7	9	9	0.028	0.043	0.035				0.26	0.432	0.48^{+}	0.25^{+}
	B	"	23.2	9	8	0.069	0.000	0.035				0.13		0.48^{+}	0.38^{+}
2	D	PH2	23.7	8	8	0.007	0.028	0.017				0.24		0.404	0.16
	K	" (control)	24.3	57	57	0.416	0.426	0.421				0.40	0.469	-	-
	N	" *	24.8	11	11	0.104	0.088	0.096				0.16	0.576	0.325	0.24
	E	"	25.3	5	7	- 0.144	- 0.038	- 0.091				0.21		0.512	0.19
3	2A	L14	31.3	9	11	0.000	0.097	0.049				0.26		0.62^{+}	0.41^{+}
	C	" (control)	31.7	60	59	0.884	0.783	0.833				0.53, 0.47	1.239	-	-
	L	" *	32.1	10	12	- 0.058	0.036	- 0.011				0.29	0.760	0.68^{+}	0.38^{+}
	B	*	32.4	14	13	-	-	-				-	-	-	-
4	D	PI3	32.7	10	10	0.172	0.136	0.154				0.26		0.543	0.37
	K	" (control)	33.1	60	58	0.757	0.636	0.697				0.63	0.656	-	-
	N	" *	33.5	9	9	0.104	0.086	0.095				0.26	0.764	0.602	0.37
	E	"	33.8	10	11	0.137	0.176	0.157				0.34		0.540	0.29
5	3A	PI3	36.5	6	9	-	-	-				-			
	C	" (control)	36.6	56	55	0.627	0.649	0.638				0.63	0.734	-	-
	L	" *	36.6	8	6	0.027	- 0.025	0.001				0.32	0.788	0.637	0.31
	B	"	36.7	8	9	0.010	0.058	0.034				0.34		0.604	0.29
6	D	PH2	36.8	8	8	- 0.002	0.014	0.006				0.29		0.644	0.24
	K	" (control)	36.8	57	57	0.631	0.669	0.650				0.53	0.787	-	-
	N	" *	36.9	6	6	- 0.0.74	- 0.066	- 0.070				0.29	0.854	0.720	0.24
	E	"	36.9	8	9	-	-	-				-			
7	COV	PP	14.9	8	7	0.080	0.057	0.068	0.082	0.051	0.067	0.09		0.202	0.12
	COF	" (control)	15.1	58	56	0.264	0.277	0.270	-	-	-	0.21	0.202	-	-
	COW	"	15.2	8	8	0.058	0.060	0.059	0.089	0.075	0.082	0.08		0.211	0.13
	COX	"	15.3	13	15	0.216	0.191	0.200	0.109	0.132	0.120	0.16	-	0.066	0.05
8	COR	PO	15.5	7	7	0.010	0.027	0.018	0.062	0.051	0.056	0.08		0.287	0.112
	COE	" (control)	15.6	64	63	0.283	0.327	0.305	0.166	0.170	0.168	0.24	0.194	-	-
	COS	"	15.7	7	7	0.002	0.009	0.005	0.012	0.032	0.022	0.00		0.300	0.146
	COT	"	15.9	14	17	0.239	0.287	0.263	0.167	0.165	0.166	0.16		0.042	0
9	COK	PI5	17.4	8	8	0.202	0.189	0.195	0.139	0.143	0.141	0.16	0.360	0.068	0.041
	COC	" (control)	17.4	61	61	0.229	0.297	0.263	0.182	0.183	0.182	0.18	0.175	-	-
	COL	"	17.5	12	12	0.182	0.173	0.177	0.117	0.115	0.116	0.13	0.303	0.086	0.066
	COM	"	17.5	19	20	0.205	0.267	0.236	0.204	0.199	0.202	0.21	0.277	0.027	0
10	CON	PH3	17.6	13	13	0.198	0.190	0.194	0.175	0.143	0.159	0.21	0.470	0.087	0.058
	COD	" (control)	17.6	65	62	0.280	0.283	0.281	0.220	0.214	0.217	0.26	0.256	-	-
	COO	"	17.7	11	11	0.153	0.144	0.149	0.142	0.124	0.133	0.21	0.429	0.132	0.084
	COP	"	17.7	18	17	0.280	0.293	0.286	0.185	0.188	0.186	0.29	0.328	0	0.031

* Indicates cylindrical axis of specimen is perpendicular to extrusion; all other specimens have their axes parallel.

\+ Using mean of I.D. and O.D. shrinkages as the control.

TABLE IV

Strength Measurements

Group	Graphite	Internal pressure test				Diametral test				Direct tensile test on unirradiated cylindrical specimens (mean and S.D. of single observation)		
		Irradiated			Unirrad.	Irradiated			Unirrad.			
		Spec. code	Creep strain at I.D. %	P $lb.in^{-2}$	Mean P and stan. dev. for 10-12 specimens	Specimen code	Creep strain at I.D. %	K_P $lb.in^{-2}$	Mean K_P of 3-4 specimens	No. of specs	Strain to fracture, %	U.T.S. $lb.in^{-2}$
7	PP	COX COW	0.07 0.21	2480 1860	1360 ± 180	COF COV	0 0.20	5380 4050	2940	8	0.19 ± 0.04	1590 ± 260
8	PO	COE COR	0 0.29	3410 3250	1740 ± 120	COT COS	0.04 0.30	5460 5530	3940	8	0.25 ± 0.09	2030 ± 530
9	PI5	COM COK	0.03 0.07	2360 2680	1180 ± 90	COC COL	0 0.09	5750 4040	3400	8	0.19 ± 0.06	1170 ± 200
10	PH3	COP COO	0 0.13	2230 2140	1320 ± 240	COD CON	0 0.09	4080 4610	2610	3	0.15	1570
4	PI3	2K 2E 2N	0 0.54 0.60	1110? 3540 2240	1670 ± 420					17	0.30 ± 0.06	2200 ± 300
2 6	PH2 (fine radial cracks) "	IK (IN (ID (IE 3K (3D (3N	0 0.33 0.40 0.51 0 0.64 0.72	2040 140 1810 390 1940 1010 1520	890 ± 50					6*	0.22 ± 0.04	1670 ± 110

* The direct tensile test was carried out in a direction parallel to extrusion, since the material was only available in small diameter bars, and was therefore in a different direction to the pressure test where the circumferential stress acted in the perpendicular direction. All other direct tests were on perpendicular cut specimens.

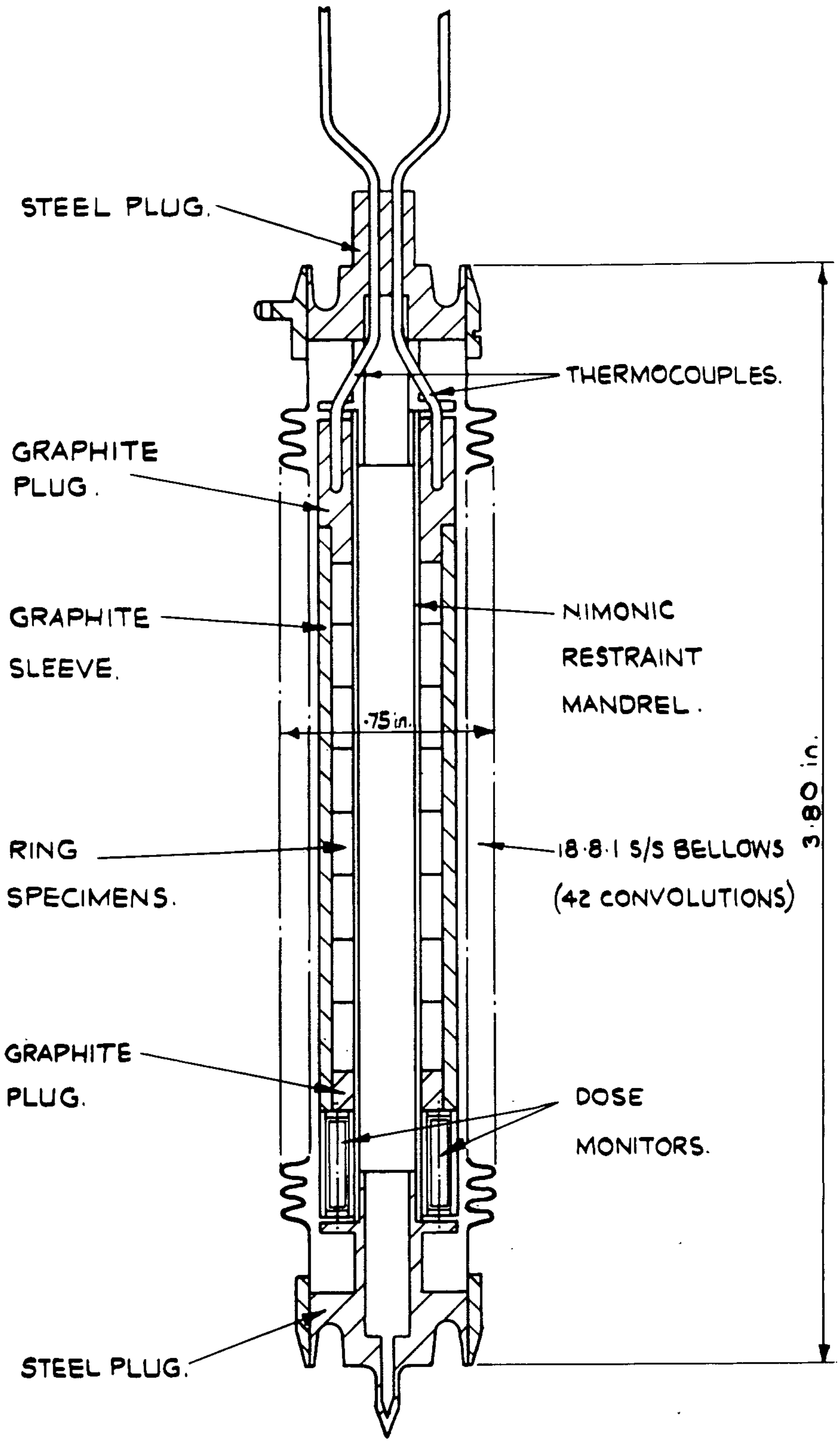

FIG.1. BR-2 CREEP CAPSULE CONTAINING GRAPHITE RING SPECIMENS UNDER TENSILE RESTRAINT.

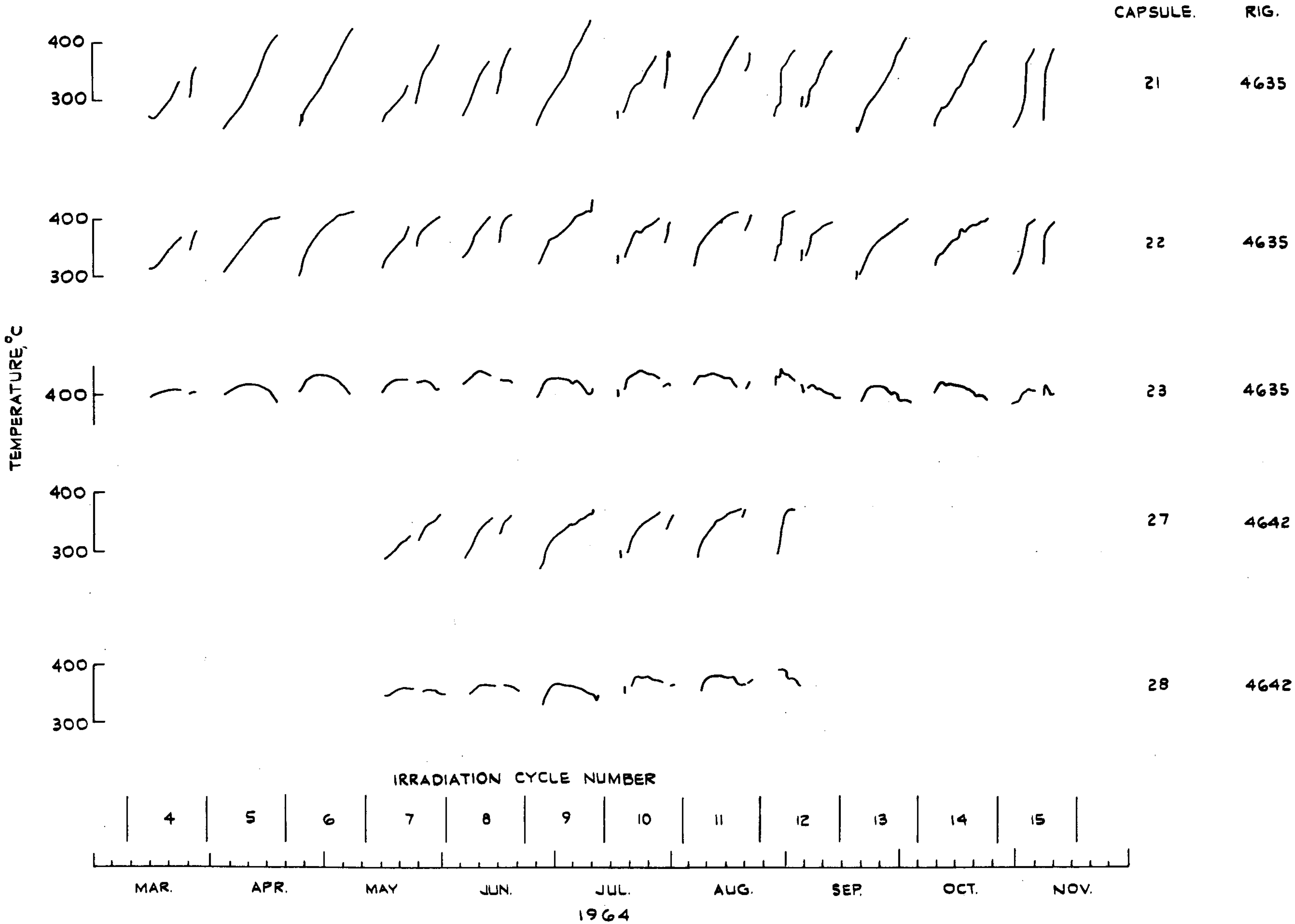

FIG. 2. IRRADIATION TEMPERATURES OF CAPSULES CONTAINING RESTRAINED SHRINKAGE SPECIMENS IN RIGS 4635 AND 4642.

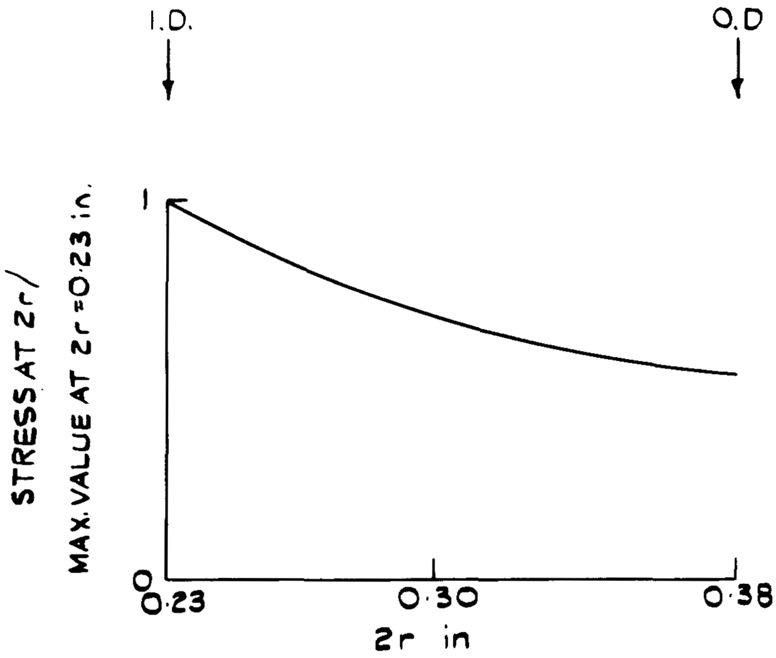

FIG.3. TENSILE HOOP STRESS DISTRIBUTION ACROSS THE WALL OF THE GRAPHITE ANNULUS.(ASSUMING ELASTIC BEHAVIOUR).

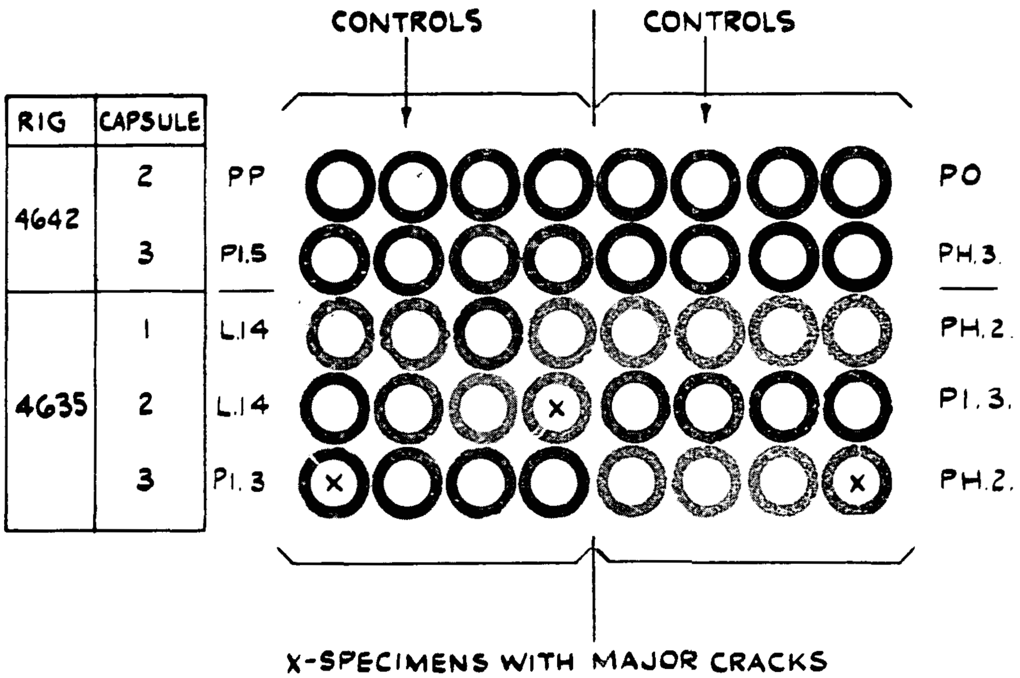

FIG.4. X-RADIOGRAPH OF GRAPHITE RING SPECIMENS FROM BR-2 RIGS 4635 AND 4642 SHOWING 3 RESTRAINED SPECIMENS WITH MAJOR CRACKS.

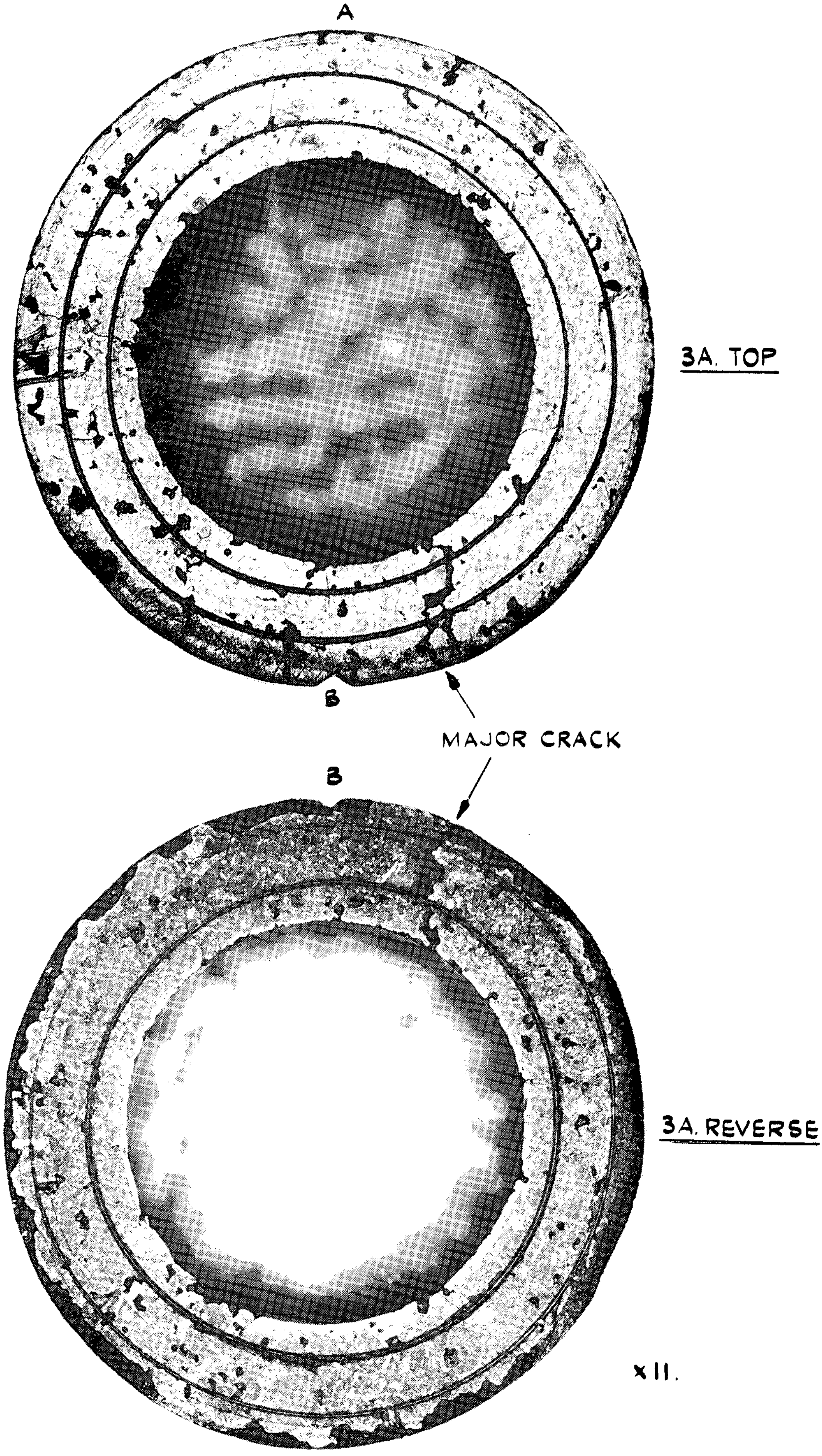

FIG.5a. SURFACES OF RESTRAINED Pl. 3. SPECIMEN SHOWING A MAJOR CRACK PASSING THROUGH THE WALL. (1 OF 3 SUCH SPECIMENS).

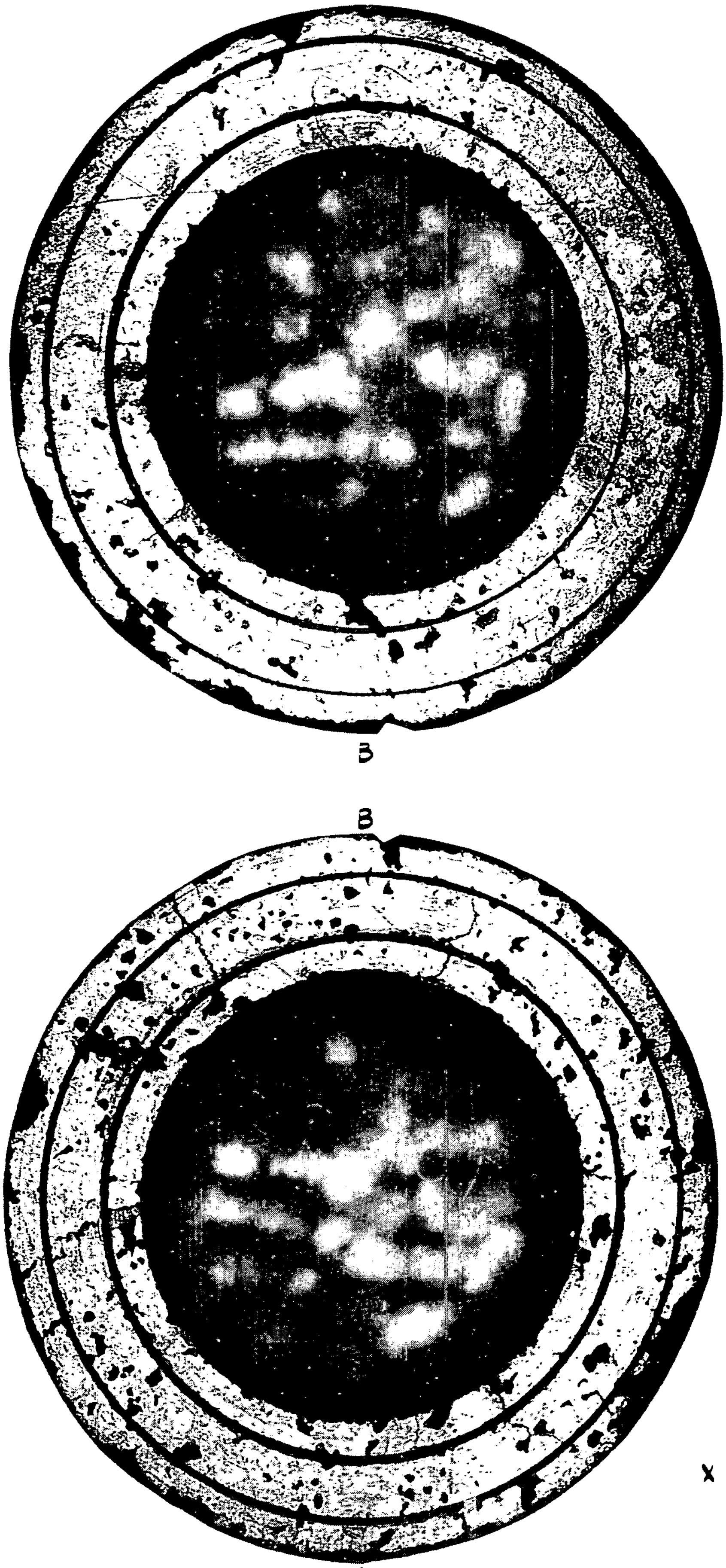

B

3B. TOP

B

3B. REVERSE.

X 11

A

FIG. 5b. SURFACES OF A RESTRAINED P1.3 SPECIMEN (0·60% AT I.D.)

SHOWING A TYPICAL FINE CRACK PATTERN.

A

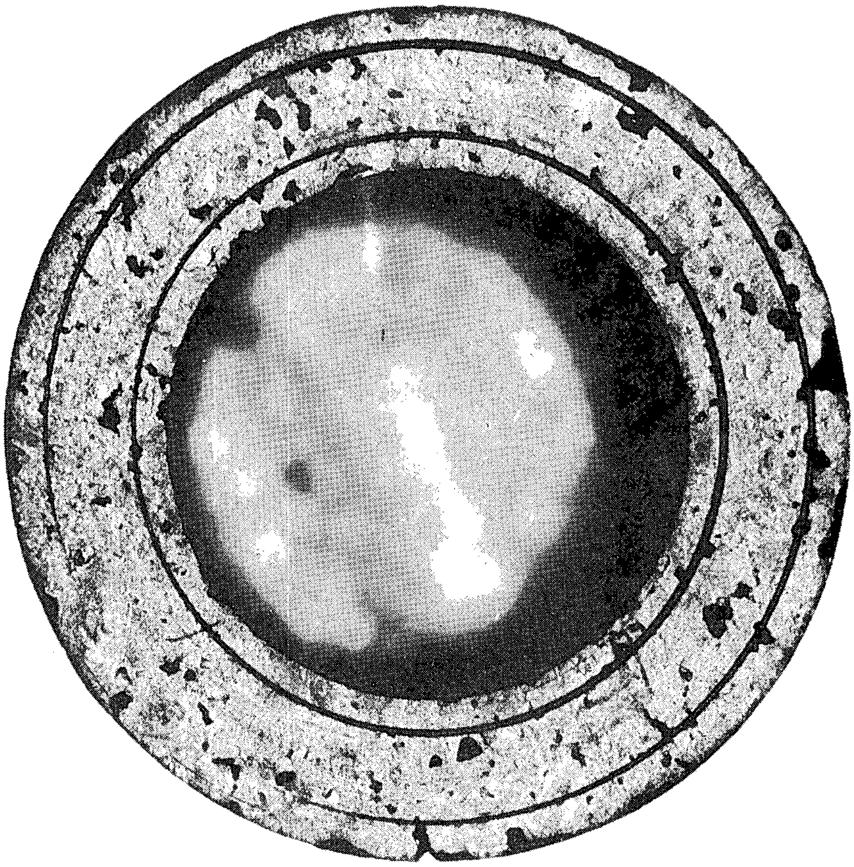

2D. TOP

B

B

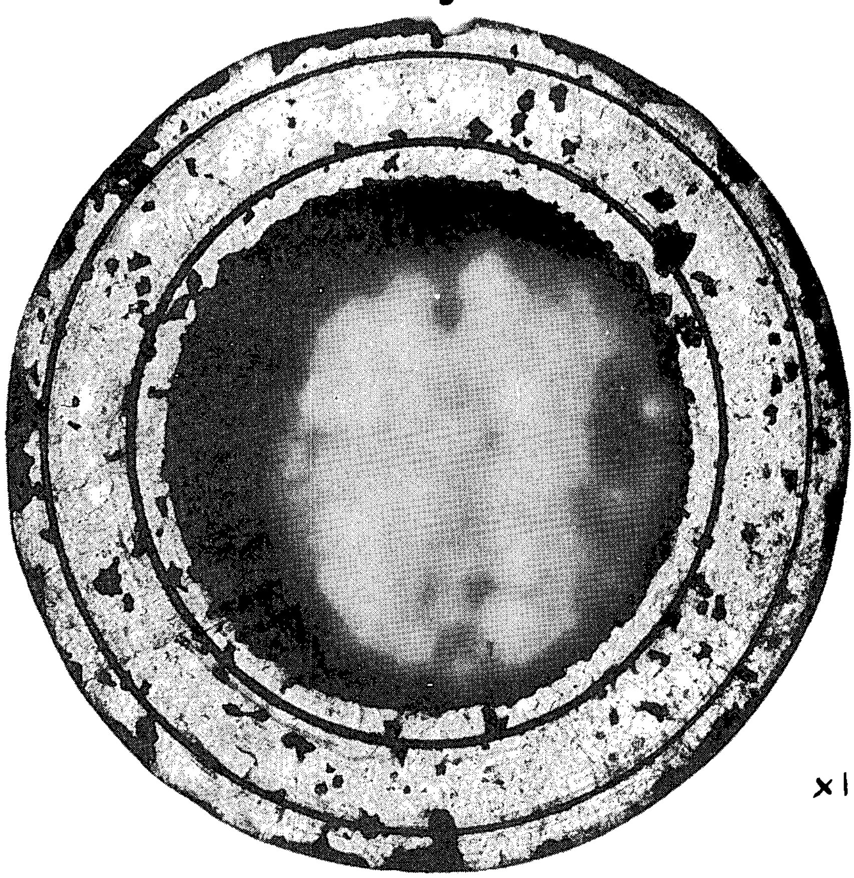

2D. REVERSE

x11

A

FIG. 5c. SURFACES OF A RESTRAINED P1.3 SPECIMEN (0·54 % AT I.D) WITH NO CRACKS.

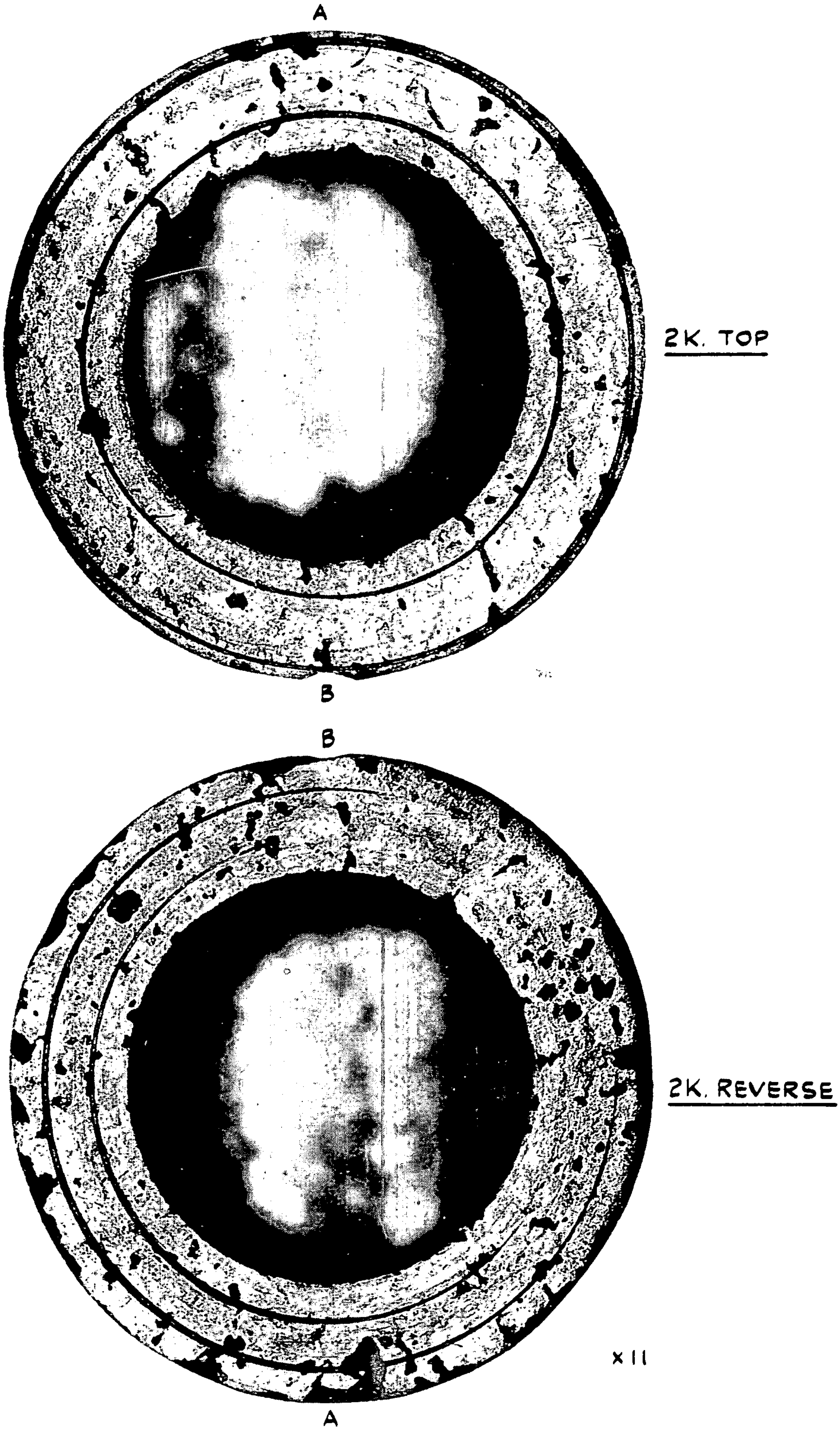

FIG. 5d. SURFACES OF AN UNRESTRAINED P1.3 CONTROL SPECIMEN.

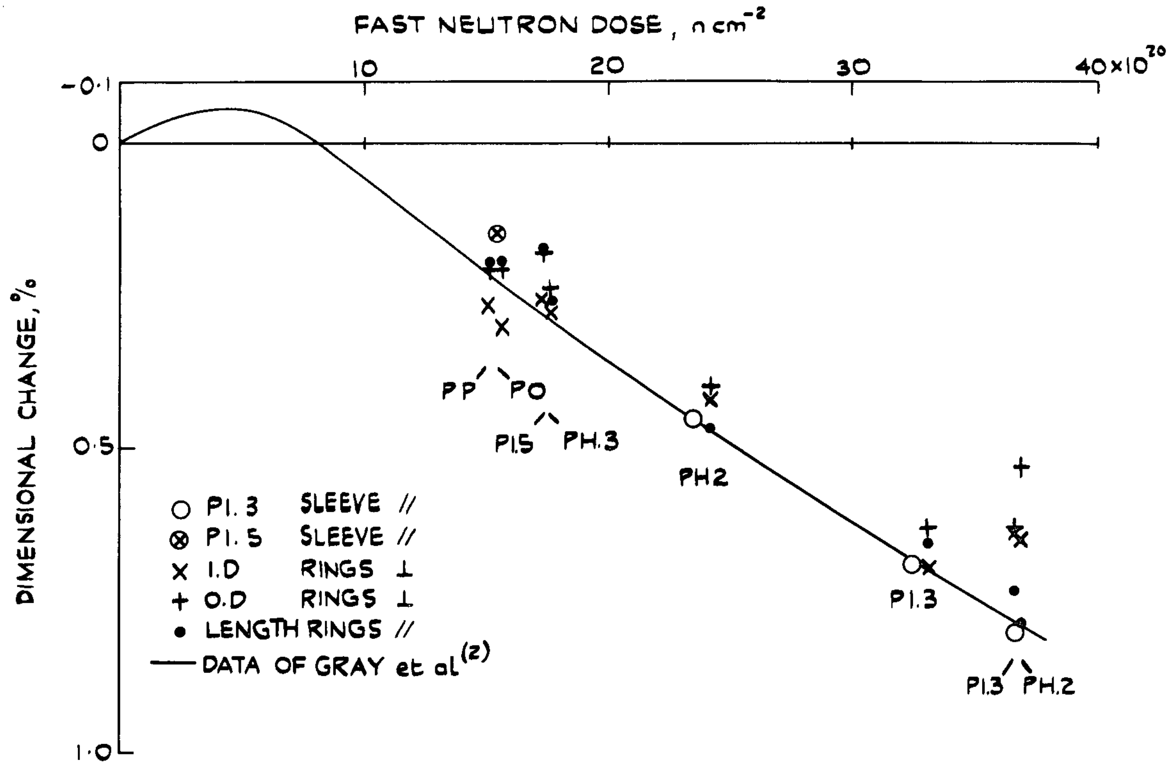

FIG.6. MEASUREMENTS ON UNRESTRAINED ISOTROPIC GRAPHITE RINGS AND OUTER SLEEVES COMPARED WITH OTHER BR-2 DATA.

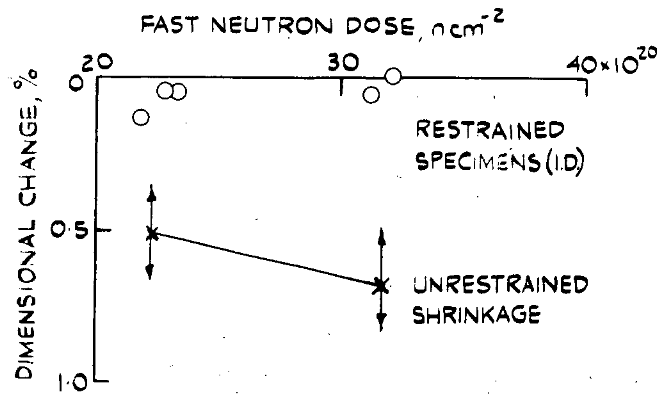

FIG. 10. DIMENSIONAL CHANGE AT THE INNER DIAMETER OF RESTRAINED P.G.A. GRAPHITE SPECIMENS (PERPENDICULAR TO EXTRUSION) COMPARED WITH UNRESTRAINED CONTROLS.

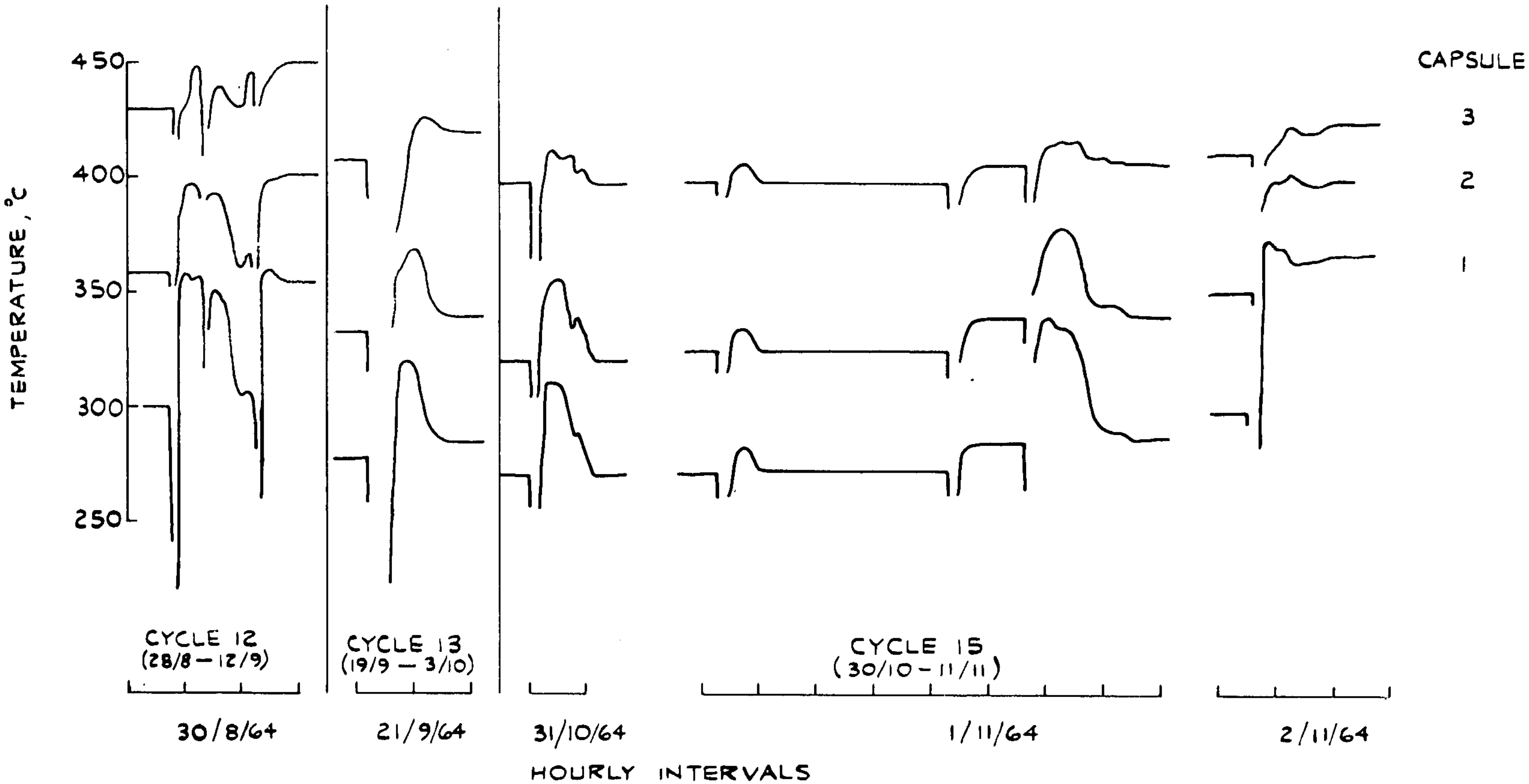

FIG. 12. INSTANTANEOUS TEMPERATURE TRANSIENTS IN RIG 4635.